



FULL PAPER

Chemo-selective reduction of nitro and nitrile compounds using Ni nanoparticles immobilized on hyperbranched polymer-functionalized magnetic nanoparticles

Seyed Jamal Tabatabaei Rezaei  | Asemeh Mashhadi Malekzadeh | Sima Poulaei |
Ali Ramazani  | Hossein Khorramabadi

Department of Chemistry, Faculty of Science, University of Zanjan, PO Box 45195-313, Zanjan, Iran

Correspondence

Seyed Jamal Tabatabaei Rezaei,
Department of Chemistry, Faculty of Science, University of Zanjan, PO Box 45195-313, Zanjan, Iran.
Email: sjt.rezaei@znu.ac.ir

The nitro and nitrile groups in aromatic and aliphatic compounds containing various reducible substituents such as carboxylic acid, ketone, aldehyde and halogen are selectively reduced to the corresponding amines in water as a green solvent with excellent yields by employing NaBH_4 in the presence of $\text{Fe}_3\text{O}_4@PAMAM/Ni(0)-b\text{-PEG}$ nanocatalyst. The morphology and structural features of the catalyst were characterized using various microscopic and spectroscopic techniques. The designed catalyst system because of it being covered with hydrophilic polymers is soluble in a wide range of solvents (e.g. water and ethanol) and suitable for immobilizing and stabilizing Ni nanoparticles in aqueous mediums. In addition, the catalyst can be easily recovered from a reaction mixture by applying an external magnetic field and can be reused up to six runs without significant loss of activity.

KEYWORDS

magnetic nanocatalyst, Ni nanoparticles, nitro and nitrile compounds, reduction

1 | INTRODUCTION

Following early attempts to obtain superior catalysts that were soluble in the reaction solvent, but could be precipitated on addition of a second solvent, chemists turned their attention to dendrimers. Dendrimers are highly branched molecules that are defined by three components: a central core, an interior dendritic structure (the branches), the 'branches' of which emanate from a core, and an exterior surface with functional surface groups. Dendrimers can be synthesized with different cores and terminal end groups.^[1-4] Dendrimers can be precipitated from solution, or, if large enough, removed using membrane filters. Poly(amido amine) (PAMAM) dendrimers are symmetric and adopt a relatively spherical shape for this reason, and are used in many different materials science and biotechnology applications. The

end groups of PAMAM dendrimers increase the solubility of the dendrimers, which is important for keeping reaction conditions relatively consistent when investigating the use of dendrimers in catalysis.^[5,6] Three structures for a catalyst delivery system have been investigated, namely the core of the dendrimer as the single catalytic unit,^[7] the dendritic box (intermediate positions within a dendrimer)^[8] and the terminal ends of the dendrimer that covalently bind to catalytic units.^[9-13] There are many examples of the use of functionalized dendrimers in catalysis of reactions including Heck couplings,^[14-16] decarboxylation,^[17] oxidation,^[18] reduction,^[19] Michael addition^[20] and so on.

In dendritic magnetic catalysis, dendrimers have been used as templates to encapsulate magnetic nanoparticles (MNPs) such as magnetite (Fe_3O_4) or maghemite ($\gamma\text{-Fe}_2\text{O}_3$). The incorporation of dendritic layers onto

MNPs led to a significant increase in the number of functional groups on the MNPs surface, allowing better stabilization of catalytic units.^[21–23] These catalysis systems were highly active, dispersible and recoverable using an external magnet, which results in conservation of energy, cheaper target products and sustainable and green chemistry.^[21,24]

Amines are important building blocks for the synthesis of pharmaceuticals, polymers, dyes, anti-foam agents, corrosion inhibitors, surfactants and agrochemicals and as intermediates for material science.^[25–29] However, due to the importance of amines in various industries, it is essential to develop new and efficient methods for their preparation.^[30–33] Although there are several methods to prepare amines, most of them are not suitable for commodity chemical production because of the formation of waste materials.^[34] For example, the catalytic reductions of nitro groups in the presence of metal complexes, metal sulfides or metal powder have various practical drawbacks, such as toxic by-products and difficulty in reuse.^[35,36] And the reduction of nitriles with LiAlH_4 and NaBH_4 often leads to a mixture of primary, secondary and tertiary amines.^[37,38] In these cases, a variety of transition metals including Co, Ni, Au, Cu, Rh, Pd and Pt have been immobilized on different supports (C, TiO_2 , SiO_4 , Al_2O_3 and so on), displaying a high potential towards the facile reduction of nitrile/nitro compounds using various reducing agents, such as H_2 , NaBH_4 , $\text{N}_2\text{H}_4 \cdot \text{H}_2\text{O}$ and so on.^[39–46] These catalytic systems constitute a major task for the development of green synthetic methodologies and are of importance in organic chemistry. Recently, extensive studies have been done on the reduction of nitrile/nitro compounds to corresponding amine derivatives using low-cost non-noble metals (e.g. Ni, Co, Fe and Cu metals or oxides).^[47–52]

To take advantage of these characteristics and also as a part of our ongoing research programme on the design of new catalysts for the development of useful and green synthetic methodologies,^[15,16,53–59] herein, we report a dendritic magnetic catalyst based on Ni(0) nanoparticles, an inexpensive non-noble metal, for selective hydrogenation of nitro and nitrile compounds in the presence of various reducible substituents such as carboxylic acid, ketone, aldehyde and halogen to the respective amines using NaBH_4 as the reducing agent in the aqueous phase. The catalyst is designed with an aim to combine the superior supporting property of PAMAM-*b*-PEG hyperbranched polymer to effectively immobilize and stabilize Ni nanoparticles in aqueous medium with the magnetic property of Fe_3O_4 nanoparticles for simple catalyst separation and therefore to improve catalyst reusability (Scheme 1). The synthesized Fe_3O_4 @PAMAM/Ni(0)-*b*-

PEG nanocatalyst remained soluble in various polar organic and aqueous solvents, but could be simply separated from reaction solutions by applying an external magnetic field.

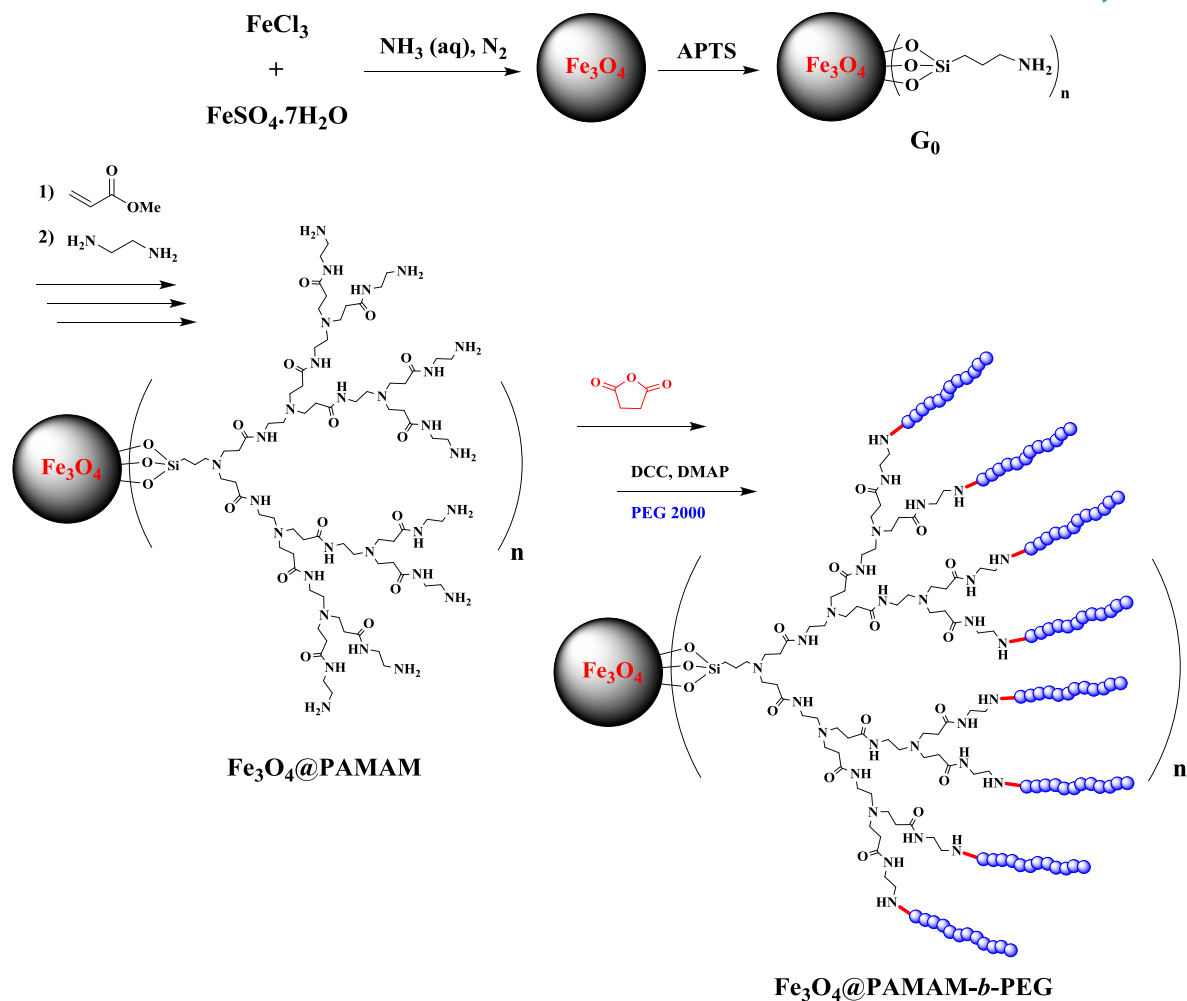
2 | EXPERIMENTAL

2.1 | Reagents and materials

FeCl_3 , 4-dimethylaminopyridine (DMAP), *N,N'*-dicyclohexylcarbodiimide (DCC), succinic anhydride, dichloromethane (DCM), 25% ammonia solution (NH_3), polyethylene glycol (PEG) with average molecular weight of 2000 g mol^{-1} and molecular sieve were purchased from Merck Chemical Co. $\text{FeSO}_4 \cdot 7\text{H}_2\text{O}$, 3-aminopropyltrimethoxysilane (APTS), methyl acrylate, toluene, tetrahydrofuran (THF), dimethylsulfoxide (DMSO) and ethylenediamine were obtained from Sigma-Aldrich. All chemicals were of analytical grade and used without purification, except for PEG which was purified by azeotropic distillation with dry toluene and DCM, dried over phosphorus pentoxide (P_2O_5) and distilled. Toluene was dried by refluxing over sodium and distilled just prior to use.

2.2 | Instrumentation

Fourier transform infrared (FT-IR) spectra were recorded with a Jasco 6300 FT-IR spectrometer. The spectra were measured in the $400\text{--}4000 \text{ cm}^{-1}$ region with samples dispersed in KBr pellets. A Shimadzu XRD-6000 X-ray diffractometer with $\text{Cu K}\alpha$ radiation (wavelength = 0.154056 nm) was used for X-ray analysis. Phase identification was performed by matching peak positions and relative intensities to reference JCPDS files. The Rietveld refinement of the X-ray diffraction (XRD) patterns was performed using TOPAS (version 4.1) software. The ^1H NMR spectra were recorded with a Bruker (Karlsruhe, Germany) DRX-250 Avance spectrometer at 250.0 MHz , and deuterated chloroform was used as a solvent. Thermogravimetric analysis (TGA) was carried out using a thermogravimetric analyser (TGA Q500) up to 800 C in air at a ramp rate of $10 \text{ }^\circ\text{C min}^{-1}$. The magnetic properties of samples were determined at room temperature using vibrating sample magnetometry (VSM; Meghnatis Kavir Kashan Co., Kashan, Iran). The size and morphological characterization of the particles was carried out using a Zeiss-EM10C transmission electron microscopy (TEM) instrument operating at 80 kV . Ultrasonic generation was carried out with a TECNO-GAZ Tecna 6 (input: $50\text{--}60 \text{ Hz/305 W}$), with uniform sonic waves to disperse materials in solvents.



SCHEME 1 Synthesis of Fe₃O₄@PAMAM-*b*-PEG

2.3 | Synthesis of APTS-coated MNPs

The MNPs were prepared according to our previous work.^[60] Briefly, 3 mmol of FeSO₄·7H₂O and 6 mmol of FeCl₃ were dissolved in 100 ml of deionized water under nitrogen atmosphere with vigorous stirring at 80 °C. Then 120 ml of aqueous ammonia solution (1.5 M) was added dropwise to this hot solution with stirring over a period of 15 min. The colour of the solution turned from dark orange to black immediately. Stirring was continued for a further 30 min followed by cooling to room temperature. The precipitate was washed three times with deionized water and twice with ethanol. Surface modification of Fe₃O₄ was performed with APTS.^[55,61] The magnetite nanoparticles (1 g) were added to 300 ml of ethanol and sonicated with an ultrasonicator for 15 min. Then, 4 ml of APTS and 4 ml of deionized water were added to the dispersion under nitrogen atmosphere. The mixture was stirred with a mechanical stirrer at room temperature for 7 h. The resulting black precipitate was separated by magnetic decantation and washed with ethanol several

times. The obtained nanoparticles modified with APTS are called G₀ generation.

2.4 | Preparation of Fe₃O₄@PAMAM

First-, second- and third-generation PAMAM dendrimers were synthesized on the amino-functionalized MNPs. Methyl acrylate/methanol solution (20%, v/v) was added (200 ml) to the amine-functionalized Fe₃O₄ nanoparticles (4 g), and the suspension was sonicated with an ultrasonicator for 15 min and then was stirred at ambient temperature under nitrogen atmosphere for 5 days. The particles were then collected magnetically and rinsed with methanol five times by magnetic separation. After rinsing, ethylenediamine/methanol solution (80 ml; 50%, v/v) was then added to the ester-functionalized Fe₃O₄ nanoparticles (4 g) and the suspension was sonicated for 15 min and then was stirred at ambient temperature under nitrogen atmosphere for 4 days. The particles were rinsed with methanol five times by magnetic separation. The

preferred number of generations from 1 to 3 (G_1 – G_3) was achieved by repetition of the stepwise growth of dendrimers using methyl acrylate and ethylenediamine.

After the synthesis, to calculate the amount of free primary amines in the periphery of the dendrimers, the titration method was used.^[62] Typically, 0.1 g of $Fe_3O_4@PAMAM$ nanoparticles was suspended in 20 ml of 0.01 M HCl aqueous solution and stirred at room temperature for 24 h. The particles were then collected magnetically and washed well with distilled water. The filtrate and washings were collected. The unreacted HCl was determined by titration against a standard Na_2CO_3 solution with the use of a pH meter. A blank titration was also carried out. From these values, the amount of amino groups per gram of the nanoparticles was calculated.

2.5 | Preparation of $Fe_3O_4@PAMAM-COOH$

To a suspension of $Fe_3O_4@PAMAM$ nanoparticles (1 g, 1.2 mmol NH_2 groups as calculated by titration) dispersed in 30 ml of dimethylformamide (DMF), succinic anhydride (4 g) in DMF (10 ml) was added dropwise under sonication. The reaction was continued for about 48 h with continuous stirring. The particles were finally recovered by magnetic concentration and washed thoroughly with ethanol.

2.6 | Preparation of $Fe_3O_4@PAMAM-b-PEG$

In a 100 ml flask with a magnetic stirring bar, PEG 2000 (3.6 mmol, 6.5 g), DMAP (4.2 mmol, 0.5 g) and $Fe_3O_4@PAMAM-COOH$ nanoparticles (1 g, 1.2 mmol COOH groups) were added in anhydrous DCM (30 ml). After the flask was cooled to 0°C, a diluted solution of DCC (3.6 mmol, 0.7 g) in 20 ml of dry DCM was added dropwise over 1 h. The reaction mixture was stirred at 0°C for another 1 h and then at room temperature for 48 h. The nanoparticles were then collected magnetically and rinsed with DCM and then ethanol.

2.7 | Synthesis of nickel nanoparticles immobilized on $Fe_3O_4@PAMAM-b-PEG$ ($Fe_3O_4@PAMAM/Ni(0)-b-PEG$)

Aqueous solutions of nickel(II) chloride hexahydrate (0.5 g in 3 ml) and $Fe_3O_4@PAMAM-b-PEG$ (1 g in 10 ml) were mixed and placed in an ultrasonic bath for 10 min to well disperse metal ions in the dendritic (PAMAM) shell of the nanoparticles. Then the mixture was stirred at room temperature for 8 h, and the reduction

was carried out with the addition of 5 ml of an aqueous solution of $NaBH_4$ (0.01 M) to the mixture and stirring at room temperature for 1 h. The $Fe_3O_4@PAMAM-b-PEG$ -supported Ni(0) nanoparticles were magnetically separated, washed well with water and ethanol (2 × 50 ml) and dried under vacuum at 50 °C for 4 h.

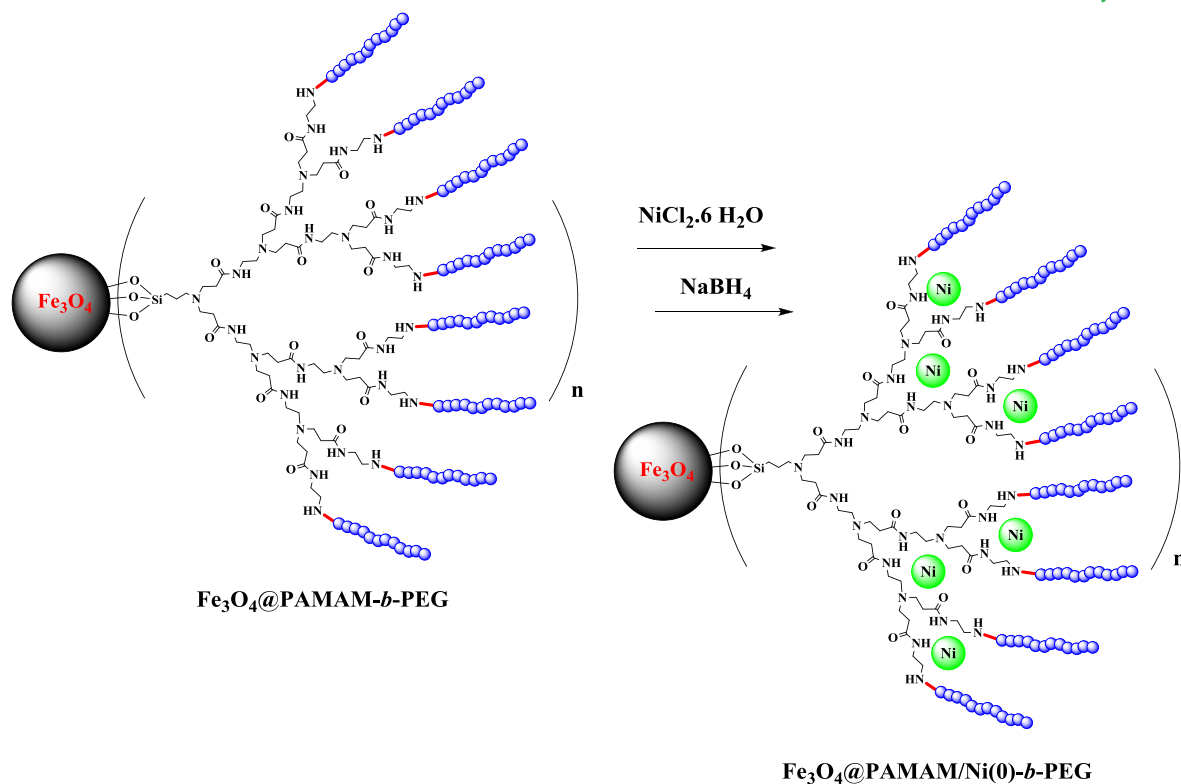
2.8 | General procedure for hydrogenation of nitro and nitrile compounds with $Fe_3O_4@PAMAM/Ni(0)-b-PEG$ as catalyst

An amount of 1 mmol of nitro or nitrile compound was added to 1 ml of distilled water and then 0.002 g of ultrasonically dispersed $Fe_3O_4@PAMAM/Ni(0)-b-PEG$ catalyst (1 mol% Ni) in water (3.0 ml) was introduced to this solution. Then 1 mmol of $NaBH_4$ was added and the mixture was stirred at 40 °C. The reaction was monitored by TLC (or GC if necessary). After the completion of the reaction, the catalyst was magnetically separated, washed several times with ethanol, air dried and used directly for the next round of reactions. After separation of the catalyst, the organic phase was combined and the solvent was removed under vacuum to obtain the pure product. The conversions were determined by GC analysis. All of the products were characterized by comparison of NMR spectral data with those of authentic samples (supporting information).

3 | RESULTS AND DISCUSSION

Schemes 1 and 2 show the chemical synthesis of $Fe_3O_4@PAMAM-b-PEG$ nanoparticles and subsequent loading of nickel, respectively. Monodisperse Fe_3O_4 MNPs were initially synthesized using the co-precipitation method in basic conditions, and then coated with APTS. Consequently, the PAMAM dendrimers up to third generation were grown on the surface of APTS-coated MNPs (G_0) to obtain the $Fe_3O_4@PAMAM$ nanoparticles employing a divergent route. In order to connect PEG chains to nanoparticles, $Fe_3O_4@PAMAM$ surface was functionalized with COOH groups using succinic anhydride as shown in Scheme 1. The PEGylation process is done to enhance the water solubility of the MNPs. In the next step, a condensation reaction took place between the pre-existing acidic hydroxyl functional groups and the PEG chains. In the final step, nickel ions were introduced into $Fe_3O_4@PAMAM-b-PEG$ nanoparticles, which interact well with the nitrogen groups of the support, and subsequently their reduction with sodium borohydride (Scheme 2).

To demonstrate the successful synthesis of $Fe_3O_4@PAMAM$, FT-IR spectra were obtained, and



SCHEME 2 Synthetic routes employed for the preparation of $\text{Fe}_3\text{O}_4@PAMAM/Ni(0)-b-PEG$ MNPs

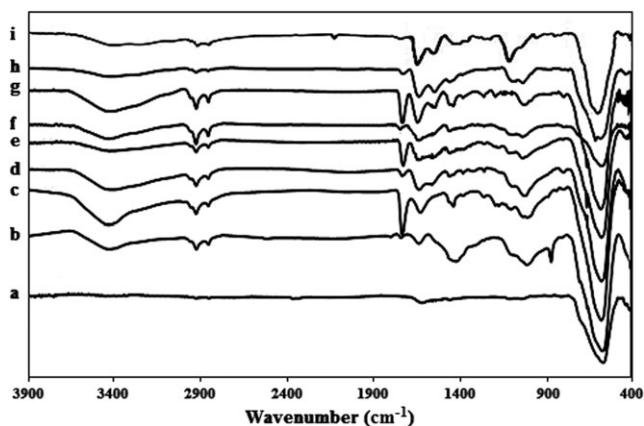


FIGURE 1 FT-IR spectra of Fe_3O_4 (a), G_0 (b), $G_{0.5}$ (c), G_1 (d), $G_{1.5}$ (e), G_2 (f), $G_{2.5}$ (g), G_3 (h) and $\text{Fe}_3\text{O}_4@PAMAM-b-PEG$ (i)

Figure 1 shows the FTIR spectra of Fe_3O_4 , G_0 and $\text{Fe}_3\text{O}_4@PAMAM$ nanoparticles. The absorption band at 570 cm^{-1} which corresponds to intrinsic stretching vibration of the metal at tetrahedral site ($\text{Fe}_{\text{tetra}}-\text{O}$) confirms the existence of magnetite nanoparticles. The peak at 997 cm^{-1} (in G_0 spectrum) is related to $\text{Si}-\text{O}-\text{Fe}$ bonds and the bands at 2919 and 2842 cm^{-1} are assigned to stretching mode of CH_2 .^[63] The broad peak at 3415 cm^{-1} is due to free NH_2 group stretching mode. The absorption band at 1734 cm^{-1} is attributed to ester groups (CO_2CH_3) in all half generation products ($G_{0.5}$, $G_{1.5}$ and

$G_{2.5}$). This band was not observed for the full generations (G_1 , G_2 and G_3), indicating that the reaction between ethylenediamine and the half-generation products had taken place. The strong bands at 1620 cm^{-1} could be assigned to stretching mode of amide groups ($-\text{CONH}-$) and the peaks at 1544 cm^{-1} are attributed to the $\text{N}-\text{H}$ bending of the secondary amide groups. Also, compared with the FTIR spectrum of $\text{Fe}_3\text{O}_4@PAMAM$, new signals related to ether units of PEG ($\text{C}-\text{O}-\text{C}$) in the range $1075-1150\text{ cm}^{-1}$ appear, indicating the successful synthesis of $\text{Fe}_3\text{O}_4@PAMAM-b-PEG$ (Figure 1i).

Figure 2 presents the XRD patterns of as-prepared Fe_3O_4 , $\text{Fe}_3\text{O}_4@PAMAM-b-PEG$ and $\text{Fe}_3\text{O}_4@PAMAM/Ni(0)-b-PEG$. The XRD patterns of $\text{Fe}_3\text{O}_4@PAMAM-b-PEG$ and $\text{Fe}_3\text{O}_4@PAMAM/Ni(0)-b-PEG$ (Figure 2b,c) show no basic change in Fe_3O_4 crystalline structure in comparison with Fe_3O_4 nanoparticles, due to their similar compositions. There is a noteworthy intensity decrease of Bragg peaks in the XRD patterns of $\text{Fe}_3\text{O}_4@PAMAM-b-PEG$ and $\text{Fe}_3\text{O}_4@PAMAM/Ni(0)-b-PEG$ compared with the XRD pattern of Fe_3O_4 (Figure 2a), which is related to the amorphous nature of coating material on the surface of the inorganic core. According to Scherrer's equation, the average crystallite size for Fe_3O_4 , $\text{Fe}_3\text{O}_4@PAMAM-b-PEG$ and $\text{Fe}_3\text{O}_4@PAMAM/Ni(0)-b-PEG$ nanoparticles was calculated as 28.5, 22.6 and 13.2 nm, respectively.^[64]

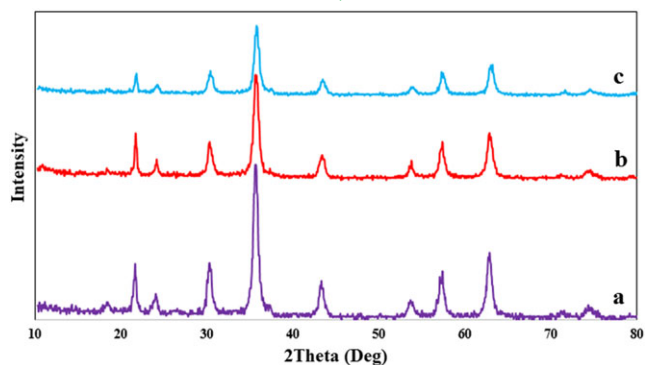


FIGURE 2 Powder XRD patterns of Fe_3O_4 (a), Fe_3O_4 @PAMAM-*b*-PEG (b) and Fe_3O_4 @PAMAM/Ni(0)-*b*-PEG (c) MNPs

The surface composition and chemical oxidation states of the prepared Fe_3O_4 @PAMAM/Ni(0)-*b*-PEG catalyst were characterized using X-ray photoelectron spectroscopy (XPS). The XPS survey scan (Figure 3a) shows

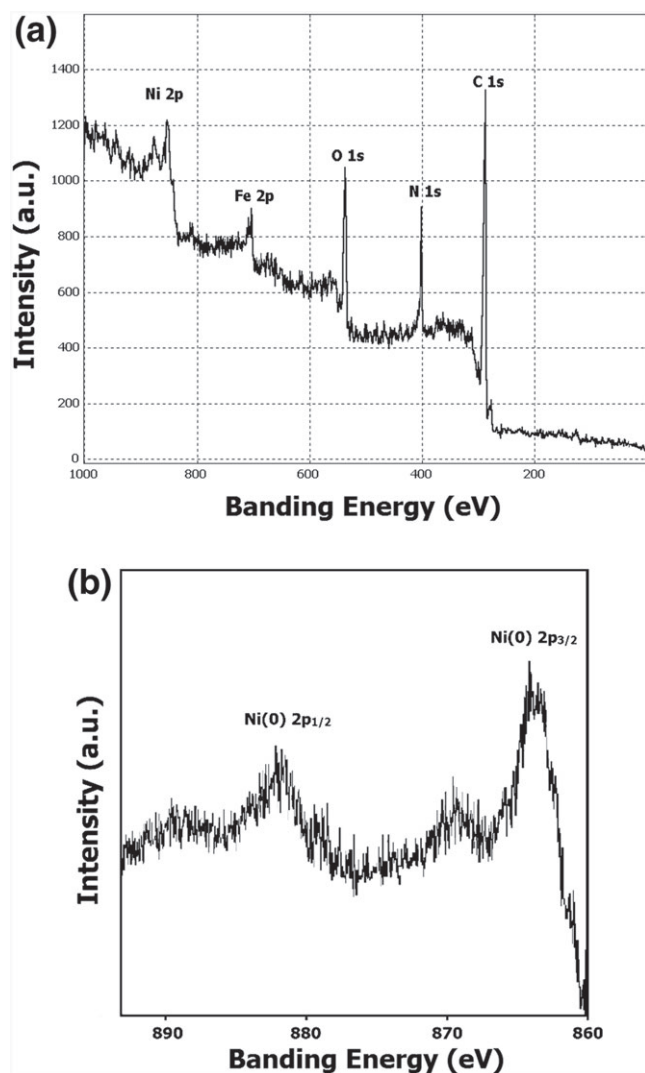


FIGURE 3 XPS survey spectrum of Fe_3O_4 @PAMAM/Ni(0)-*b*-PEG (a), and high-resolution Ni 2p XPS spectrum of Fe_3O_4 @PAMAM/Ni(0)-*b*-PEG (b)

the presence of Ni 2p signal together with Fe 2p, O 1s, N 1s and C 1s signals derived from Fe_3O_4 @PAMAM-*b*-PEG. Thus, the XPS data also confirm the presence of Ni in the prepared catalyst. The high-resolution Ni 2p XPS scan of Fe_3O_4 @PAMAM/Ni(0)-*b*-PEG catalyst is illustrated in Figure 3b which reveals the presence of Ni 2p_{3/2} and 2p_{1/2} peaks at binding energies of 863.4 and 880.75 eV, respectively. These results are consistent with those reported for metallic Ni(0) oxidation state.^[65,66]

Atomic absorption spectrometry (AAS) was used to calculate the weight percent of nickel in the catalyst. The data showed that the amount of nickel immobilized on Fe_3O_4 @PAMAM-*b*-PEG is about 15.11 wt%. TGA is a common method used to determine organic content in a sample. The TGA curve of Fe_3O_4 (Figure 4a) shows that

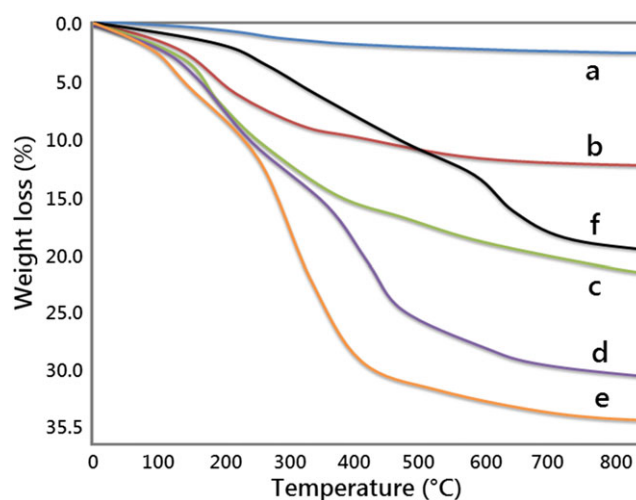


FIGURE 4 TGA curves of Fe_3O_4 (a), G_1 (b), G_2 (c) G_3 (d), Fe_3O_4 @PAMAM-*b*-PEG (e) and Fe_3O_4 @PAMAM/Ni(0)-*b*-PEG (f)

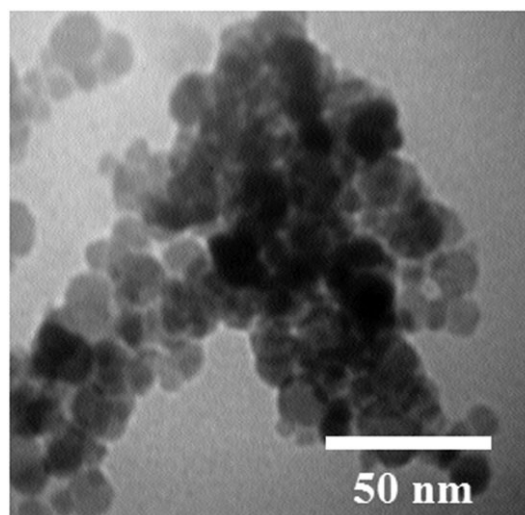


FIGURE 5 TEM image of Fe_3O_4 @PAMAM/Ni(0)-*b*-PEG nanocatalyst

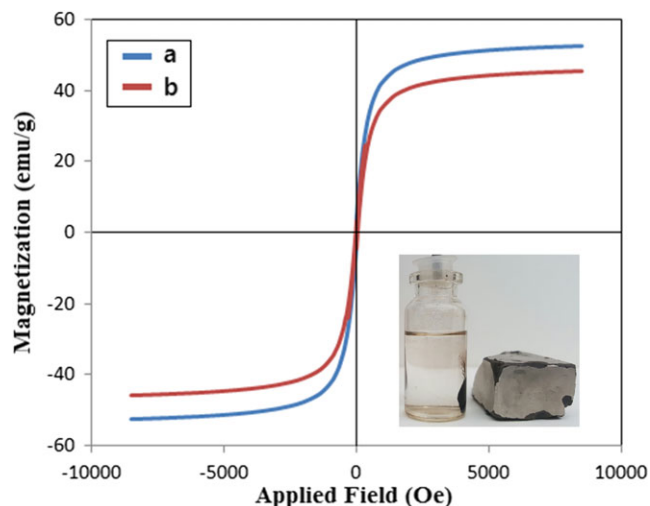


FIGURE 6 Hysteresis loops for Fe_3O_4 (a) and Fe_3O_4 @PAMAM/Ni(0)-*b*-PEG (b) at 25 °C. Inset: Digital image of magnetic separation of catalyst after reaction

the weight loss of Fe_3O_4 over the range from 20 to 800 °C is about 2.53% which might be because of the loss of residual water in the sample. The first, second and third generations of Fe_3O_4 @PAMAM and Fe_3O_4 @PAMAM-*b*-PEG had 7.1, 9.4, 9.3 and 3.73% weight losses, respectively, indicating the amount of polymer layers on the surfaces of nanoparticles. Also, comparing the TGA curves of Fe_3O_4 @PAMAM-*b*-PEG and Fe_3O_4 @PAMAM/Ni(0)-*b*-

PEG (Figure 4e and f) demonstrates that the weight percent of Ni(0) nanoparticles loaded on the surface of MNPs is about 14.97%, which is consistent with the results obtained using AAS.

It has been proved that the surface modification of nanoparticles with the polymer leads to uniform distribution and less aggregation of nanoparticles. Figure 5 shows a TEM image of the Fe_3O_4 @PAMAM/Ni(0)-*b*-PEG nanocatalyst. The Fe_3O_4 @PAMAM/Ni(0)-*b*-PEG nanospheres are clearly evident in TEM image with an average diameter of *ca* 15 nm. TEM observations indicate that Ni nanoparticles are dispersed into the hyperbranched polymers on the surface of Fe_3O_4 . This is due to the presence of a large number of nitrogen heteroatoms, as anchoring sites, on the surface of nanoparticles (Scheme 2).

The magnetic behaviours of the synthesized nanoparticles were measured at room temperature using VSM analysis. The hysteresis loops of the samples are shown in Figure 6. The saturation magnetizations were found to be 52.56 and 44.74 emu g^{-1} for Fe_3O_4 and Fe_3O_4 @PAMAM/Ni(0)-*b*-PEG, respectively, which means that the catalyst can be easily recycled from a reaction solution using an external magnetic field (inset of Figure 6). However, the magnetization of PAMAM-*b*-PEG-grafted Fe_3O_4 is slightly lower than the unmodified Fe_3O_4 nanoparticles, indicating the coating formation on the surface of the Fe_3O_4 likely affects the magnetic ability.^[67]

TABLE 1 Optimization of reaction conditions for reduction of 4-nitroaniline with Fe_3O_4 @PAMAM/Ni(0)-*b*-PEG as catalyst system^a

$\text{H}_2\text{N}-\text{C}_6\text{H}_4-\text{NO}_2 \xrightarrow[\text{Solvent, NaBH}_4]{\text{Fe}_3\text{O}_4\text{@PAMAM/Ni(0)-b-PEG}} \text{H}_2\text{N}-\text{C}_6\text{H}_4-\text{NH}_2$					
Entry	Solvent	Catalyst amount (Ni(0) content, mol%)	Time (h)	Temp. (°C)	Yield (%) ^b
1	H ₂ O	—	2	40	—
2	H ₂ O	0.1	2	40	36
3	H ₂ O	0.5	2	40	78
4	H ₂ O	1.5	2	40	95
5	H ₂ O	1	0.5	40	50
6	H ₂ O	1	1	40	79
7	H ₂ O	1	3	40	94
8	H ₂ O	1	2	40	94
9	H ₂ O	1	2	30	89
10	H ₂ O	1	2	25	76
11	H ₂ O–EtOH (1/2)	1	2	40	88
12	EtOH	1	2	40	57
13	Toluene	1	2	40	36
14	THF	1	2	40	41
15	DMSO	1	2	40	62

^aReaction conditions: 1 mmol of 4-nitroaniline and 1 mmol of NaBH₄.

^bIsolated yield.

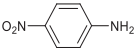

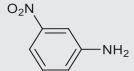
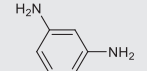
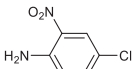
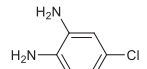
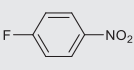
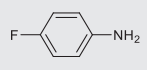
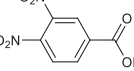
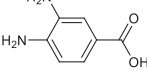
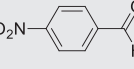
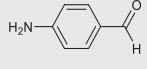
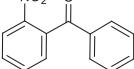
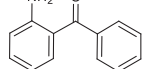
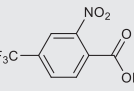
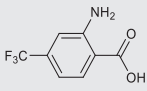
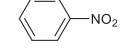
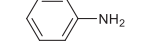
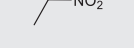
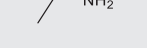
After characterization of the $\text{Fe}_3\text{O}_4@\text{PAMAM}/\text{Ni}(0)-b\text{-PEG}$ catalyst, we attempted to evaluate its catalytic activity for the reduction of nitro and nitrile compounds. We first used 4-nitroaniline as a model compound to demonstrate $\text{Fe}_3\text{O}_4@\text{PAMAM}/\text{Ni}(0)-b\text{-PEG}$ catalysis for the hydrogenation of nitro compounds and to obtain the optimum reaction conditions. To optimize the amount of the catalyst, the model reaction was performed with various amounts of the catalyst in water at 40°C (Table 1, entries 1–4). Within 2 h and with 1 mol% of nickel, 94% yield of *p*-phenylenediamine was obtained (Table 1, entry 8). In contrast, increasing the amount of the catalyst to 1.5 mol% did not affect the yield considerably (Table 1, entry 4). However, the reaction did not happen in the absence of catalyst (Table 1, entry 1). The effect of temperature and reaction time

(Table 1, entries 5–10) was also investigated by carrying out the model reaction at different temperatures and times, and the highest yield was obtained at 40°C and 2 h (Table 1, entry 8).

We examined the catalytic reactions at 40°C in various solvents including water, water–ethanol (1/2), ethanol, toluene, THF and DMSO, and determined water to be the best solvent to convert 4-nitroaniline to *p*-phenylenediamine. The hydrophobic nature of the dendrimer interior void space ensures that the reactants tend to collect at those areas rather than the water solvent. Since nickel nanoparticles as catalyst also exist in these spaces, it is expected that an efficient catalytic reaction occurs.

Under optimal catalytic reaction conditions, we studied the reduction reactions of various functionalized nitro

TABLE 2 Reduction reaction of nitro compounds with $\text{Fe}_3\text{O}_4@\text{PAMAM}/\text{Ni}(0)-b\text{-PEG}$ as catalyst system^a

Entry	Nitro compound	Product	Yield (%) ^b
1			94
2			93
3			90
4			91
5			95
6			97
7			95
8			96
9			91
10			89

^aReaction conditions: 1 mmol nitro compound, 1 mmol NaBH_4 , 3 ml H_2O , $\text{Fe}_3\text{O}_4@\text{PAMAM}/\text{Ni}(0)-b\text{-PEG}$ (1 mol% Ni(0)) at 40 °C for 2 h.

^bIsolated yield.

substrates to the respective amines (Table 2). Some of these amines, such as chloro-substituted anilines, are industrially and biologically important. *m*-Nitroaniline and *p*-nitroaniline were cleanly reduced to the corresponding anilines (Table 2, entries 1 and 2). The Chloro- and fluoro-substituted nitroarenes (Table 2, entries 3 and 4) were selectively reduced to the respective haloaromatic amines without any dehalogenation, which is often encountered with several procedures such as hydrogenation.^[68–71] An analysis of the results of Table 2 shows that the best yields were obtained with substrates containing electron-withdrawing groups (entries 5–8). The ketone, carboxylic acid, and aldehyde functionalities present in the aromatic ring also remained unaffected during reduction of the corresponding nitrobenzenes by this procedure (entries 5–8). Nitroethane was successfully reduced to ethanamine using this catalyst system (entry 10).

Encouraged by the excellent results obtained using $\text{Fe}_3\text{O}_4@\text{PAMAM}/\text{Ni}(0)\text{-}b\text{-PEG}$ as a catalyst for the reduction of nitro compounds in aqueous media, we set out to optimize the reaction conditions for the reduction of nitrile compounds in aqueous media. To obtain the

optimum reaction conditions for the hydrogenation of nitrile compounds we used 4-pyridinecarbonitrile as a model compound (Table 3). As can be seen (entries 1–4), the yield of the product increased with increasing amounts of catalyst. In contrast, increasing the amount of the catalyst to 1.5 mol% did not affect the yield considerably (Table 3, entry 4). According to the results of the effect of temperature and reaction time on the reduction of 4-pyridinecarbonitrile, the highest yield was obtained at 95 °C and 1 h (Table 3, entry 8). After the amount of catalyst, reaction temperature and time were optimized, the influence of solvent on the reaction was studied in the next step (Table 3, entries 11–15). It was found that the best system was water as solvent using 1 mol% of catalyst at 95 °C and a time of 1 h.

Because benzylamine compounds are important biologically, the reduction of benzonitriles is a key issue. The results in Table 4 show that benzonitriles with one or more electron-withdrawing groups on the aromatic ring could be efficiently converted to the corresponding amines in high yields under optimum conditions (Table 4, entries 1–3). In contrast, benzonitriles with electron-donating groups (Table 4, entries 4–6) converted to

TABLE 3 Optimization of reaction conditions for reduction of 4-pyridinecarbonitrile with $\text{Fe}_3\text{O}_4@\text{PAMAM}/\text{Ni}(0)\text{-}b\text{-PEG}$ as catalyst system^a

Entry	Solvent	Catalyst amount (Ni(0) content, mol%)	Time (h)	Temp. (°C)	Yield (%) ^b
1	H ₂ O	—	1	95	—
2	H ₂ O	0.1	1	95	29
3	H ₂ O	0.5	1	95	62
4	H ₂ O	1.5	1	95	89
5	H ₂ O	1	0.5	95	46
6	H ₂ O	1	1.5	95	89
7	H ₂ O	1	2	95	90
8	H ₂ O	1	1	95	89
9	H ₂ O	1	1	60	61
10	H ₂ O	1	1	25	38
11	H ₂ O–EtOH (1/2)	1	1	Reflux	81
12	EtOH	1	1	Reflux	62
13	Toluene	1	1	95	18
14	THF	1	1	Reflux	30
15	DMSO	1	1	95	76

^aReaction conditions: 1 mmol of 4-pyridinecarbonitrile and 1 mmol of NaBH_4 .

^bIsolated yield.

TABLE 4 Reduction reaction of nitrile compounds with $\text{Fe}_3\text{O}_4@\text{PAMAM}/\text{Ni}(0)\text{-}b\text{-PEG}$ as catalyst system^a

Entry	Nitrile compound	Product	Yield (%) ^b
1			97
2			95
3			96
4			88
5			90
6			92
7			89
8			94
9			87
10			88

^aReaction conditions: 1 mmol nitrile compound, 1 mmol NaBH_4 , 3 ml H_2O , $\text{Fe}_3\text{O}_4@\text{PAMAM}/\text{Ni}(0)\text{-}b\text{-PEG}$ (1 mol% $\text{Ni}(0)$) at 95 °C for 1 h.

^bIsolated yield.

the corresponding amines in lower yields. The lower yield of 2-methoxybenzonitrile (Table 4, entry 4) than 4-methoxybenzonitrile (Table 3, entry 5) is attributed to the steric hindrance around the reduction site. It is necessary to mention that many developed catalytic systems are not able to reduce aliphatic nitriles even under extended reflux conditions.^[72–74] This inability is related to the deprotonation of the hydrogen α to the nitrile with these reagents and thus halting the reduction. However, our catalytic system is able to reduce aliphatic nitriles in good yields (Table 4, entries 9 and 10).

The stability and recyclability of semi-heterogeneous catalysts for practical applications, especially in industry, are of great importance. For this reason, the cyclic stability of the as-prepared $\text{Fe}_3\text{O}_4@\text{PAMAM}/\text{Ni}(0)\text{-}b\text{-PEG}$

catalysts was also studied by monitoring the catalytic activity during successive cycles of nitro and nitrile compound reduction reactions. Therefore, the reduction reactions of 4-nitroaniline and 4-pyridinecarbonitrile were carried out under optimum conditions for up to six cycles. After each experimental run, CH_2Cl_2 was added and the catalyst was easily separated from the product by attaching an external magnet onto the reaction vessel. Also, the catalyst was washed several times with absolute ethanol and dried under vacuum and reused directly for the next round of reactions. As shown in Figure 7, the $\text{Fe}_3\text{O}_4@\text{PAMAM}/\text{Ni}(0)\text{-}b\text{-PEG}$ catalyst was still highly active with an average yield 93.2% for nitro and 88% for nitrile compounds after six cycles, clearly illustrating the high stability and excellent reusability of the catalyst. Furthermore, in another test, $\text{Fe}_3\text{O}_4@\text{PAMAM}/\text{Ni}(0)\text{-}b\text{-PEG}$ was magnetically separated from the reaction mixture after *ca* 50% conversion at the reaction temperature. Further reaction of the filtrate under optimum conditions did not proceed significantly. AAS of the filtrate also confirmed that the Ni content in the solution was below the detection limit. Therefore, we may conclude that any Ni nanoparticles that leached into the reaction mixture are not an active homogeneous catalyst and that the observed catalysis is truly heterogeneous in nature.

Comparison of the results with those for various other non-noble metal catalysts employed earlier for the reduction of nitro and nitrile groups in aromatic and aliphatic compounds indicates that our synthesis methodology (Table 5, entry 1) involves greener and milder reaction conditions as well as better catalytic activity compared to other reported catalysts. These systems require longer reaction time (entries 2, 3 and 6), higher amount of additives (entries 3, 4, 5 and 6), difficulties of catalyst separation from the reaction mixture

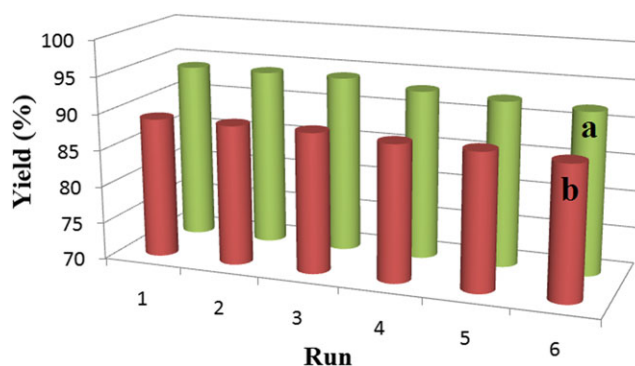


FIGURE 7 Effect of recycling on the catalytic activity and productivity of $\text{Fe}_3\text{O}_4@\text{PAMAM}/\text{Ni}(0)\text{-}b\text{-PEG}$ in reactions of (a) 4-nitroaniline (green) and (b) 4-pyridinecarbonitrile (red)

TABLE 5 Comparison of results for reduction of nitrobenzene (a) and benzonitrile (B) with those for some other reported non-noble metal catalysts

Entry	Catalyst	Reactant	Solvent	Catalyst/non-noble metal content (mol%)	Additive/amount (mmo)l	Temp. (°C)	Time (min)	Yield (%)	Ref.	
1	Fe ₃ O ₄ @PAMAM/ Ni(0)-b-PEG	A	Water	Ni(0)/1	NaBH ₄ /1	—	40	120	91	Present work
		B	Water	Ni(0)/1	NaBH ₄ /1	—	95	60	94	
2	NiNPs@Fe ₃ O ₄ - SiO ₂ -P4VP	A	Not tested							[66]
		B	Water	Ni(0)/1	NaBH ₄ /1	—	90	120	88	
3	Fe ₃ O ₄ -Ni MNPs	A	Glycerol	Ni(0)/8.85	KOH/2	—	80	180	94	[75]
		B	Not tested							
4	Ni-PAMAM- PVAm/SBA-15	A	Water	Ni(0)/10	NaBH ₄ /3	—	25	10	98	[65]
		B	Not tested							
5	NiNPs/PVP	A	Water	Ni(0)/20	N ₂ H ₄ ·H ₂ O/excess	—	25	75	99	[48]
		B	Not tested							
6	CoNPs/PVP	A	Water	Co(0)/20	N ₂ H ₄ ·H ₂ O/excess	—	25	300	50	[48]
		B	Not tested							

P4VP = poly(4-vinylpyridine); PVAm = polyvinylamine; PVP = polyvinylpyrrolidone.

(entries 5 and 6) and higher amounts of catalyst (entries 3–6).^[48,65,66,75]

4 | CONCLUSIONS

We have demonstrated that the semi-heterogeneous catalytic system Fe₃O₄@PAMAM/Ni(0)-b-PEG is very efficient for the selective reduction of nitro and nitrile groups in aromatic and aliphatic compounds containing various reducible substituents such as carboxylic acid, ketone, aldehyde and halogen to the corresponding amines in water as a green solvent. The dendritic and amphiphilic layers on Fe₃O₄ MNPs with unique properties such as large surface area and multi-functionality cause an enhancement of the dispersibility of the MNPs in polar solvents and stabilize the Ni nanoparticles. Other notable advantages of this methodology include high stability and reusability of catalyst, clean reactions, easy workup, short reaction times and cost-effectiveness. All these features make this method an attractive and useful alternative in organic synthesis.

ACKNOWLEDGEMENT

We are grateful to the University of Zanjan Research Council for partial support of this study.

ORCID

Seyed Jamal Tabatabaei Rezaei  <http://orcid.org/0000-0002-1065-752X>

Ali Ramazani  <http://orcid.org/0000-0003-3072-7924>

REFERENCES

- [1] D. Patton, Y. C. Sweeney, T. McCarthy, S. Hillier, *Antimicrob. Agents Chemother.* **2006**, *50*, 1696.
- [2] Y. Cheng, Z. Xu, M. Ma, T. Xu, *J. Pharm. Sci.* **2008**, *97*, 123.
- [3] H. Kobayashi, S. Kawamoto, T. Saga, N. Sato, A. Hiraga, T. Ishimori, J. Konishi, K. Togashi, M. W. Brechbiel, *Magn. Reson. Med.* **2001**, *46*, 781.
- [4] C. L. Jackson, H. D. Chanzy, F. P. Booy, B. J. Drake, D. A. Tomalia, B. J. Bauer, E. J. Amis, *Macromolecules* **1998**, *31*, 6259.
- [5] P. K. Maiti, T. Çain, G. Wang, W. A. Goddard, *Macromolecules* **2004**, *37*, 6236.
- [6] M. Tülü, A. E. Bozdogan, A. S. Ertürk, *PAMAM Dendrimers: Design, Synthesis, Characterization and Analytical Applications*, Walter de Gruyter **2017**.
- [7] C.-M. Lo, H.-F. Chow, *J. Org. Chem.* **2009**, *74*, 5181.
- [8] J. F. Jansen, E. de Brabander-van den Berg, E. Meijer, *Science* **1994**, *266*, 1226.
- [9] L. Balogh, D. A. Tomalia, *J. Am. Chem. Soc.* **1998**, *120*, 7355.
- [10] M. Ooe, M. Murata, T. Mizugaki, K. Ebitani, K. Kaneda, *J. Am. Chem. Soc.* **2004**, *126*, 1604.
- [11] M. Pittelkow, K. Moth-Poulsen, U. Boas, J. B. Christensen, *Langmuir* **2003**, *19*, 7682.
- [12] S.-K. Oh, Y. Niu, R. M. Crooks, *Langmuir* **2005**, *21*, 10209.
- [13] R. Narayanan, M. A. El-Sayed, *J. Phys. Chem. B* **2004**, *108*, 8572.
- [14] L. K. Yeung, R. M. Crooks, *Nano Lett.* **2001**, *1*, 14.
- [15] M. R. Nabid, Y. Bide, S. J. Tabatabaei Rezaei, *Appl. Catal. A* **2011**, *406*, 124.
- [16] S. J. Tabatabaei Rezaei, A. Shamseddin, A. Ramazani, A. Mashhadi Malekzadeh, P. Azimzadeh Asiabi, *Appl. Organometal. Chem.* **2017**, e3707.
- [17] K. Vassilev, W. T. Ford, *J. Polym. Sci. A* **1999**, *37*, 2727.

- [18] P. P. Zweni, H. Alper, *Adv. Synth. Catal.* **2004**, *346*, 849.
- [19] V. Chechik, R. M. Crooks, *J. Am. Chem. Soc.* **2000**, *122*, 1243.
- [20] M. Zhao, Y. Liu, R. M. Crooks, D. E. Bergbreiter, *J. Am. Chem. Soc.* **1999**, *121*, 923.
- [21] D. Wang, D. Astruc, *Chem. Rev.* **2014**, *114*, 6949.
- [22] Q. M. Kainz, O. Reiser, *Acc. Chem. Res.* **2014**, *47*, 667.
- [23] N. V. Kuchkina, E. Y. Yuzik-Klimova, S. A. Sorokina, A. S. Peregudov, D. Y. Antonov, S. H. Gage, B. S. Boris, L. Z. Nikoshvili, E. M. Sulman, D. G. Morgan, *Macromolecules* **2013**, *46*, 5890.
- [24] V. Polshettiwar, R. Luque, A. Fihri, H. Zhu, M. Bouhrara, J.-M. Basset, *Chem. Rev.* **2011**, *111*, 3036.
- [25] S. A. Lawrence, *Amines: Synthesis, Properties and Applications*, Cambridge University Press **2004**.
- [26] N. Ono, *The Nitro Group in Organic Synthesis*, Wiley-VCH, New York **2001** 30.
- [27] N. Gospodinova, L. Terlemezyan, *Prog. Polym. Sci.* **1998**, *23*, 1443.
- [28] A. G. MacDiarmid, *Synth. Met.* **1997**, *84*, 27.
- [29] A. W. Czarnik, *ACS Conf. Ser.* **1996**, 20036.
- [30] Ö. F. Erdem, L. Schwartz, M. Stein, A. Silakov, S. Kaur-Ghumaan, P. Huang, S. Ott, E. J. Reijerse, W. Lubitz, *Angew. Chem.* **2011**, *123*, 1475.
- [31] P. Moschou, J. Wu, A. Cona, P. Tavladoraki, R. Angelini, K. Roubelakis-Angelakis, *J. Exp. Botany* **2012**, *63*, 5003.
- [32] S. Santra, P. R. Andreana, *Angew. Chem. Int. Ed.* **2011**, *50*, 9418.
- [33] J. Yu, F. Shi, L.-Z. Gong, *Acc. Chem. Res.* **2011**, *44*, 1156.
- [34] F. Ullmann, W. Gerhartz, Y. S. Yamamoto, F. T. Campbell, R. Pfefferkorn, J. F. Rounsaville, *Ullmann's Encyclopedia of Industrial Chemistry*, VCH **1988**.
- [35] G. Wienhöfer, M. Baseda-Krüger, C. Ziebart, F. A. Westerhaus, W. Baumann, R. Jackstell, K. Junge, M. Beller, *Chem. Commun.* **2013**, *49*, 9089.
- [36] G. Wienhöfer, I. Sorribes, A. Boddien, F. Westerhaus, K. Junge, H. Junge, R. Llusar, M. Beller, *J. Am. Chem. Soc.* **2011**, *133*, 12875.
- [37] P. S. Liu, *J. Org. Chem.* **1987**, *52*, 4717.
- [38] T. T. Shawe, C. J. Sheils, S. M. Gray, J. L. Conard, *J. Org. Chem.* **1994**, *59*, 5841.
- [39] F. Cárdenas-Lizana, M. A. Keane, *J. Mater. Sci.* **2013**, *48*, 543.
- [40] G. Blanita, M. D. Lazar, *Micro Nanosyst.* **2013**, *5*, 138.
- [41] P. Kukula, V. Gabova, K. Koprivova, P. Trtik, *Catal. Today* **2007**, *121*, 27.
- [42] D. Segobia, A. Trasarti, C. Apesteguía, *Appl. Catal. A* **2012**, *445*, 69.
- [43] J. Krupka, J. Drahonsky, A. Hlavackova, *React. Kinet., Mech. Catal.* **2013**, *108*, 91.
- [44] A. J. Yap, A. F. Masters, T. Maschmeyer, *ChemCatChem* **2012**, *4*, 1179.
- [45] Y. Li, Y. Gong, X. Xu, P. Zhang, H. Li, Y. Wang, *Catal. Commun.* **2012**, *28*, 9.
- [46] M. Chatterjee, M. Sato, H. Kawanami, T. Yokoyama, T. Suzuki, T. Ishizaka, *Adv. Synth. Catal.* **2010**, *352*, 2394.
- [47] C. Bornschein, S. Werkmeister, B. Wendt, H. Jiao, E. Alberico, W. Baumann, H. Junge, K. Junge, M. Beller, *Nat. Commun.* **2014**, *5*.
- [48] R. K. Rai, A. Mahata, S. Mukhopadhyay, S. Gupta, P.-Z. Li, K. T. Nguyen, Y. Zhao, B. Pathak, S. K. Singh, *Inorg. Chem.* **2014**, *53*, 2904.
- [49] M. R. Nabid, Y. Bide, Z. Habibi, *RSC Adv.* **2015**, *5*, 2258.
- [50] F. A. Westerhaus, R. V. Jagadeesh, G. Wienhöfer, M.-M. Pohl, J. Radnik, A.-E. Surkus, J. Rabeah, K. Junge, H. Junge, M. Nielsen, *Nat. Chem.* **2013**, *5*, 537.
- [51] D. Cantillo, M. Baghbanzadeh, C. O. Kappe, *Angew. Chem. Int. Ed.* **2012**, *51*, 10190.
- [52] S. Farhadi, M. Kazem, F. Siadatnasab, *Polyhedron* **2011**, *30*, 606.
- [53] H. Ahmar, A. R. Fakhari, M. R. Nabid, S. J. T. Rezaei, Y. Bide, *Sens. Actuators B* **2012**, *171–172*, 611.
- [54] H. Hosseini, S. J. T. Rezaei, P. Rahmani, R. Sharifi, M. R. Nabid, A. Bagheri, *Sens. Actuators B* **2014**, *195*, 85.
- [55] M. R. Nabid, Y. Bide, E. Aghaghafari, S. J. T. Rezaei, *Catal. Lett.* **2014**, *144*, 355.
- [56] M. R. Nabid, S. J. Tabatabaei Rezaei, M. Abedi, *Synth. Commun.* **2010**, *41*, 191.
- [57] M. R. Nabid, S. S. Taheri, R. Sedghi, S. J. T. Rezaei, *Macromol. Res.* **2011**, *19*, 280.
- [58] S. J. T. Rezaei, M. R. Nabid, S. Z. Hosseini, M. Abedi, *Synth. Commun.* **2012**, *42*, 1432.
- [59] S. J. Tabatabaei Rezaei, *J. Iranian Chem. Soc.* **2017**, *14*, 585.
- [60] A. M. Malekzadeh, A. Ramazani, S. J. T. Rezaei, H. Niknejad, *J. Colloid Interface Sci.* **2017**, *490*, 64.
- [61] S. Khoei, N. Abedini, *Polymer* **2014**, *55*, 5635.
- [62] M. P. Kapoor, Y. Kasama, T. Yokoyama, M. Yanagi, S. Inagaki, H. Nanbu, L. R. Juneja, *J. Mater. Chem.* **2006**, *16*, 4714.
- [63] J. Estelrich, E. Escribano, J. Queralt, M. Busquets, *Int. J. Mol. Sci.* **2015**, *16*, 8070.
- [64] R. Liu, Y. Ren, Y. Shi, F. Zhang, L. Zhang, B. Tu, D. Zhao, *Chem. Mater.* **2007**, *20*, 1140.
- [65] R. J. Kalbasi, F. Zamani, *RSC Adv.* **2014**, *4*, 7444.
- [66] M. R. Nabid, Y. Bide, M. Niknezhad, *ChemCatChem* **2014**, *6*, 538.
- [67] D. Herea, H. Chiriac, *Optoelectron Adv. Mater. Rapid Commun.* **2008**, *2*, 549.
- [68] A. M. Tafesh, J. Weiguny, *Chem. Rev.* **1996**, *96*, 2035.
- [69] C. Yu, B. Liu, L. Hu, *J. Org. Chem.* **2001**, *66*, 919.
- [70] S. K. Mohapatra, S. U. Sonavane, R. V. Jayaram, P. Selvam, *Org. Lett.* **2002**, *4*, 4297.
- [71] B. Chen, U. Dingerdissen, J. Krauter, H. L. Rotgerink, K. Möbus, D. Ostgard, P. Panster, T. Riermeier, S. Seebald, T. Tacke, *Appl. Catal. A* **2005**, *280*, 17.
- [72] C. J. Collins, G. B. Fisher, A. Reem, C. T. Goralski, B. Singaram, *Tetrahedron Lett.* **1997**, *38*, 529.
- [73] H. C. Brown, S. Kim, S. Krishnamurthy, *J. Org. Chem.* **1980**, *45*, 1.

- [74] V. Bažant, M. Čapka, M. Černý, V. Chvalovský, K. Kochloefl, M. Kraus, J. Málek, *Tetrahedron Lett.* **1968**, 9, 3303.
- [75] M. B. Gawande, A. K. Rathi, P. S. Branco, I. D. Nogueira, A. Velhinho, J. J. Shrikhande, U. U. Indulkar, R. V. Jayaram, C. A. A. Ghumman, N. Bundaleski, O. M. N. D. Teodoro, *Chem. – Eur. J.* **2012**, 18, 12628.

SUPPORTING INFORMATION

Additional Supporting Information may be found online in the supporting information tab for this article.

How to cite this article: Tabatabaei Rezaei SJ, Mashhadi Malekzadeh A, Poulaei S, Ramazani A, Khorramabadi H. Chemo-selective reduction of nitro and nitrile compounds using Ni nanoparticles immobilized on hyperbranched polymer-functionalized magnetic nanoparticles. *Appl Organometal Chem.* 2017;e3975. <https://doi.org/10.1002/aoc.3975>